UNIVERSITYOF BIRMINGHAM

University of Birmingham
Research at Birmingham

Mathematical modeling and performance study of Fischer-Tropsch synthesis of liquid fuel over cobalt-silica

Moazami, Nima; Mahmoudi, Hamid; Panahifar, Pooria; Rahbar, Kiyarash; Tsolakis, Athanasios; Wyszynski, Miroslaw

Link to publication on Research at Birmingham portal

The 7th International Conference on Applied Energy – ICAE2015

Mathematical Modeling and Performance Study of Fischer-Tropsch Synthesis of Liquid Fuel over Cobalt-Silica

Nima Moazami, Hamid Mahmoudi, Pooria Panahifar, Kiyarash Rahbar, Athanasios Tsolakis, Miroslaw L Wyszynski*

School of Mechanical Engineering, College of Engineering and Physical Sciences, The University of Birmingham, Edgbaston, Birmingham, B15 2TT, UK

Abstract

A numerical one-dimensional pseudo-homogeneous mathematical model of a fixed bed reactor for Fischer-Tropsch (FT) synthesis was developed over a simulated nitrogen-rich syngas (33% hydrogen, 17% carbon monoxide and 50% nitrogen (volume basis)), on a cobalt-silica catalyst. An algorithm was developed and the MATLAB codes were written in order to predict the product selectivity (H_2O, CO_2 and hydrocarbons i.e. CH_4, C_2, C_3, C_4 and C_{5+}) and syngas conversion (CO and H_2). In order to predict the kinetic parameters, the global search optimization subroutine (from MATLAB Global Optimization) was used. The model was fitted with experimental data at five different operating conditions with respect to conversion and selectivity. Discrimination between the model and the experiments was determined by the mean absolute relative residuals percentage (MARR %) and the value was 13.29%. The Effects of operating conditions such as reaction temperature, total pressure, flow rate and H_2/CO molar ratio were investigated on the catalytic performance of the cobalt-silica for synthesis of liquid fuel. The model was studied in the range of 200-260 °C, 1-25 bar, reduced gas flow rate (per unit mass of catalyst) of 2.4-3.6 NL g_{cat}^{-1} h^{-1} and H_2/CO = 1.75-2.75 (mole basis).

Keywords: Fixed bed reactor; Fischer-Tropsch synthesis; mathematical modeling; renewable energy; kinetic study; biofuel production

* Corresponding author. Tel: +44 121 414 4159; mobile: +44 7968 157 909
E-mail address: M.L.Wyszynski@bham.ac.uk (Miroslaw L. Wyszynski)

1. Introduction

Fischer-Tropsch (FT) synthesis comprises a system of catalytic processes that can be defined as the means to produce renewable, carbon-neutral and sustainable transportation fuels such as gasoline, diesel, jet fuel and other chemicals from synthesis gas. Converting biomass to liquid via FT synthesis has been gaining increasing attention from industry and academia because of the absence of aromatic compounds, sulfur, their high cetane number and its capability to produce globally friendly chemicals and ultra-clean fuels. In general, the synthetic biodiesel has 22% more energy per gallon and 80% less combustion emissions; compared to petroleum diesel [1, 2]. Among different solid catalysts, cobalt is considered the most favorable catalyst for the production of long-chain hydrocarbons due to its high selectivity to linear paraffins, high activity, and high resistance to deactivation [3]. To enhance the performance of the complete FT process, the development of engineering mathematical description of the reactor and kinetics model is necessary, in which detailed selectivity, conversion and product distribution can be presented. A few examples of modeling and kinetic study of a fixed bed FT reactor over cobalt catalyst were reported in the present study [4-10]. No-one has carried out mathematical modeling of a fixed bed reactor with the details of the kinetic model on Co-SiO$_2$ using a simulated nitrogen-rich syngas.

Nomenclature

a_j	pre-exponential factor of reaction 'j', [mol pa$^{-(m_j+n_j)}$ g$_{cat}^{-1}$ s^{-1}]
C_i	concentration of species 'i', [mol m^{-3}]
d_p	average particle diameter, [m]
E_j	activation energy of reaction 'j', [J mol^{-1}]
M_m	molecular weight of mixture, [g mol^{-1}]
m	partial order of the reactant with respect to hydrogen, [-]
n	partial order of the reactant with respect to carbon monoxide, [-]
p_i	partial pressure of species 'i', [bar]
p_T	total pressure, [bar]
R_j	rate of reaction 'j', [mol g$_{cat}^{-1}$ s^{-1}]
R_g	universal gas constant, 8.314 [J mol^{-1} K^{-1}]
S_i	selectivity of species 'i', [%]
T	reaction temperature, [K]
u_s	superficial fluid velocity, [m s^{-1}]
x	conversion, [%]
β	volume fraction of active site of the solid particles, [-]
δ	explicit temperature dependence factor of the pre-exponential constant, [-]
ϵ	void fraction, [-]
ρ_f	density of the fluid, [kg m^{-3}]
ρ_B	density of the bulk catalyst, [kg$_{cat}$ m^{-3}]
v_{ij}	stoichiometric coefficient of component 'i' in reaction 'j', [-]

---

2. Experimental setup

A seamless stainless steel single micro-structured vertical fixed bed reactor was used with a tube length of 52.83 cm, outer diameter of 1.90 cm and wall thickness of 0.16 cm. An in-house spherical Co catalyst and commercial silica support (Fuji Silysia Chemical Ltd) had the following specifications: silica support bulk density of 0.38 g ml^{-1}; cobalt catalyst with particle diameter; weight, surface area, water content and

pore volume of 0.15 mm, 2.0 g, 257 $m^2 g^{-1}$, 0.6 wt% and 1.20 ml g^{-1}, respectively. In this process, a simulated N_2-rich syngas bottle with 33% H_2, 17% CO and 50% N_2 (volume basis) was employed to feed into the reactor inlet. Fig. 1 indicates the Process Path Flow (PPF) of the experimental setup. The reactor was fixed in a tube furnace (with the temperature ranging from 50 to 1100 °C) in order to produce the heat zone. A cast iron jacket was installed between the furnace and reactor to provide the uniform wall temperature. A calibrated smart mass flow controller (Bronkhorst Ltd) was employed to regulate the flow rate of the syngas. The catalytic reactor bed was purged by N_2 bottle and then the catalyst was activated by employing the H_2 gas bottle. The active catalyst was put on stream for 12 hours to determine the conversion of CO, selectivity of CH_4, CO_2, and other HC products over this period of reaction time. The liquid products were separated from the gaseous stream by two liquid/gas separators. The changes in the CO_2 and CO mole fraction were monitored on-line by using a modified CO analyzer (AVL Digas 440). Gas Chromatogram Flame Ionization Detector (GC-FID) (HP 5890) was employed to analyze the HC_1-HC_8 on-line. Gas Chromatogram-Mass Spectrometry (GC-MS) (PerkinElmer [TM]) was also used to analyze the liquid products off-line.
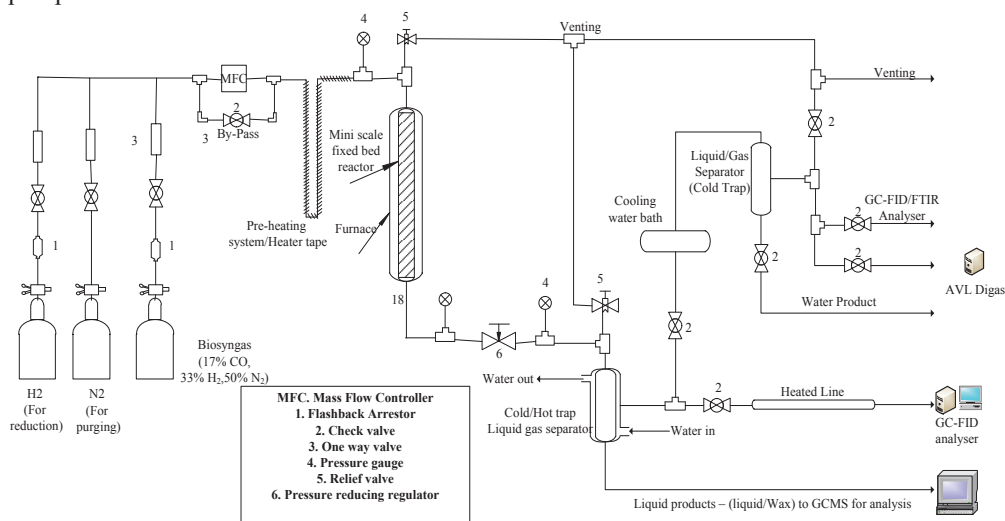
Fig. 1. Schematic diagram of the experimental setup in the present work.

3. Development of the reactor model and FT synthesis kinetic

The reaction mechanism of FT synthesis is very complex, whereby thousands of species participate in a highly coupled mode. For this reason, it is not possible to establish a reaction equation for every species by the conventional method used in reaction kinetics studies. In this study, the innumerable chemical compounds, with carbon number higher than five (C_{5+}), in the reaction system are lumped by $C_{6.05}H_{12.36}$. In order to derive the reaction kinetics model, the production rate of each species was assumed to be of the power-law form, as a function of the partial pressure of CO and H_2 components. Reaction Eqs. (1) to (8) are the proposed chemical reactions for FT synthesis over Co-SiO$_2$ in the present study. Table 1 represents the reaction kinetic parameters estimated by the model on the basis of experimental data.

$CO + 3H_2 \rightarrow CH_4 + H_2O$ (1)
$2CO + 4H_2 \rightarrow C_2H_4 + 2H_2O$ (2)
$2CO + 5H_2 \rightarrow C_2H_6 + 2H_2O$ (3)
$3CO + 7H_2 \rightarrow C_3H_8 + 3H_2O$ (4)
$4CO + 9H_2 \rightarrow n\text{-}C_4H_{10} + 4H_2O$ (5)
$4CO + 9H_2 \rightarrow i\text{-}C_4H_{10} + 4H_2O$ (6)
$6.05CO + 12.23H_2 \rightarrow C_{6.05}H_{12.36}\ (C_{5+}) + 6.05H_2O$ (7)
$CO + H_2O \rightarrow CO_2 + H_2$ (8)
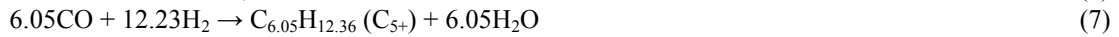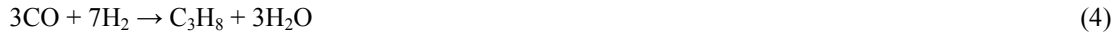
Table 1 Adjusted kinetic parameters of FT synthesis over Co/SiO_2

Reaction equation	Eq. 1	Eq. 2	Eq. 3	Eq. 4	Eq. 5	Eq. 6	Eq. 7	Eq. 8
n_j	1.04	-2.13	2.21	1.58	-1.03	-1.82	1.62	2.5
m_j	-0.27	0.59	-1.42	-0.8	1.5	2.12	-0.59	-2.05
δ_j	-0.86	0.01	-0.71	-0.13	1	1	-0.21	1
α_j	$6.56 \cdot 10^1$	$4.54 \cdot 10^{-2}$	$1.14 \cdot 10^{-3}$	$1.19 \cdot 10^{-6}$	$1.84 \cdot 10^{-1}$	$6.59 \cdot 10^{-9}$	$1.98 \cdot 10^{-8}$	$3.78 \cdot 10^{-5}$
E_j	$8.35 \cdot 10^4$	$6.50 \cdot 10^4$	$4.98 \cdot 10^4$	$3.49 \cdot 10^4$	$2.77 \cdot 10^4$	$2.57 \cdot 10^4$	$2.36 \cdot 10^4$	$5.88 \cdot 10^4$

A one-dimensional single-phase pseudo-homogeneous mathematical model was developed to simulate a single fixed bed FT reactor. A steady state operation was assumed so that there was not any change over the time including catalytic activity, selectivity and stability. The model describes the axial profiles of radially averaged concentrations, partial pressure, feed conversion and selectivity accounting for twelve species at each operating conditions. The heat transfer in this model was assumed to be isothermal. The partial pressure gradient with respect to the axial distance along the reactor length was calculated by conservation of species in Eq. (9). The continuity equation was employed to demonstrate the gas velocity profile (Eq. (10)). The chain rule was applied to the ideal gas law in order to compute the fluid density changes (Eq. (11)) in the axial dimension. The overall pressure drop (Eq. (12)) was calculated by the classical Ergun law for the fluid flow. The CO conversion was calculated by Eq. (13) and the selectivity of CO_2 and hydrocarbon products were determined by Eqs. (14) to (16). Also, Eq. (17) is the classic Arrhenius equation which is developed in order to determine the rate of consumption CO and H_2, as well as production of species. The error obtained between the model and experiential data was calculated by Eq. (18).

$$\frac{u_s}{R_g T} \frac{dp_i}{dz} = \rho_B \beta \sum_{j=1}^{NR} v_{ij} R_j - \left(\frac{p_T}{R_g T} \frac{du_s}{dz} \right)$$ (9)

$$\rho_f \frac{du_s}{dz} = -u_s \frac{d\rho_f}{dz}$$ (10)

$$\frac{d\rho_f}{dz} = \frac{d\left(\frac{p_T M_m}{R_g T} \right)}{dz} \frac{M_m}{R_g} \left[\frac{1}{T} \frac{dp_T}{dz} \right]$$ (11)

$$\frac{\partial p_T}{\partial z} = -\frac{(1-\varepsilon)^2}{\varepsilon^3} \frac{36(25/6)}{Re} \frac{u_s^2 \rho_f}{d_p}$$ (12)

$$x_i = \frac{C_{input,i} - C_{output,i}}{C_{input,i}} \times 100$$ (13)

$$S_i = \frac{C_{output,i}}{C_{input,i=CO} - C_{output,i=CO}} \times 100 \ (if \ i = CO_2) \tag{14}$$

$$S_i = \frac{C_{input,i}}{C_{input,CO} - C_{output,CO} - C_{output,CO2}} \times 100 \ (if \ i = C_1 - C_4) \tag{15}$$

$$S_{C_{5+}} = 100 - \left(S_{C_1} + S_{C_2} + S_{C_3} + S_{C_4}\right) \tag{16}$$

$$R_j = \alpha_j \left(\frac{T}{T_0}\right)^{\delta_j} \exp\left(-\frac{E_j}{RT}\right) p_{CO}^{n_j} p_{H_2}^{m_j} \tag{17}$$

$$MARR\% = \frac{1}{n} \sum_{j=1}^{NR} \left\{ \sum_{i=1}^{NC} \left| \frac{X_i^{exp} - X_i^{cal}}{X_i^{exp}} \times 100 \right| \right\} \tag{18}$$

4. Results and discussion

4.1. Model prediction

Five sets of experimental conditions at different reaction temperature, inlet total pressure and GHSV) were performed to determine the accuracy of the mathematical model and developed kinetic equations. Fig. 2 shows the predicted results and the corresponding measured data by the experiment for the proposed FT species CO, CO_2, CH_4, C_2, C_3, C_4 and C_{5+}. A parity plot (Fig. 3) indicates the accuracy of the prediction in terms of conversion and selectivity (Eq. (13) - (16)). The discrimination of the results between the model and experiments was based on the mean absolute relative residuals percentage (MARR %) error (Eq. (16)). Among the different techniques, the global search method was utilized from MATLAB Global Optimization to minimize the MARR, by adjusting the kinetic parameters. The model was fitted against the experiments satisfactorily with MARR = 13.29%.
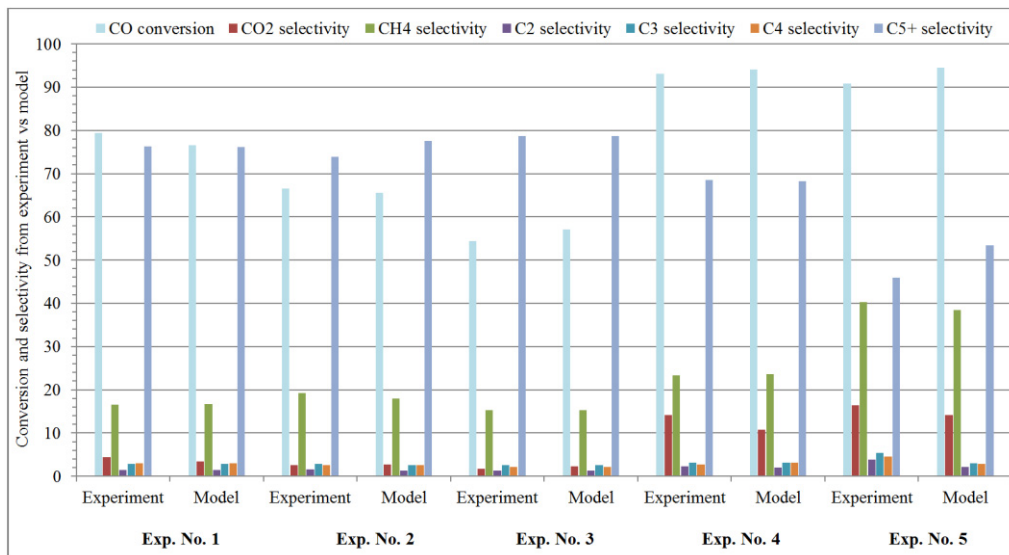

Fig. 2. Comparison of the results between model predictions and measured data with respect to CO conversion and selectivity of CO_2, CH_4, C_2, C_3, C_4 and C_{5+}; Exp. No. 1 at 230 °C, 15 bar and 2.4 NL g_{cat}^{-1} h^{-1}; Exp. No. 2 at 230 °C, 20 bar and 3 NL g_{cat}^{-1} h^{-1}; Exp. No. 3 at 230 °C, 25 bar and 3.6 NL g_{cat}^{-1} h^{-1}; Exp. No. 4 at 245 °C, 10 bar and 2.4 NL g_{cat}^{-1} h^{-1}; Exp. No. 5 at 255 °C, 10 bar and 3 NL g_{cat}^{-1} h^{-1}.
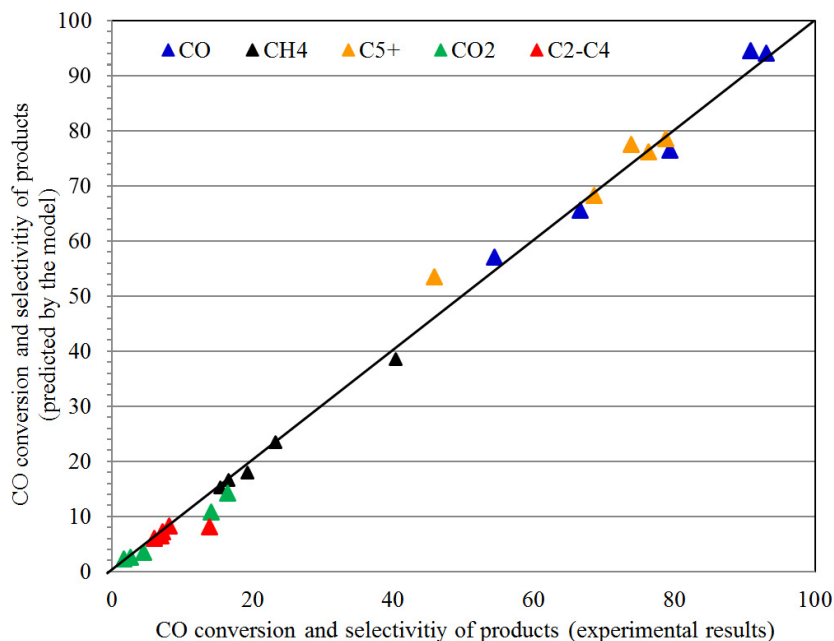
Fig. 3. Parity plot of experimental values versus calculated values for a cobalt-silica catalyst. FT synthesis species including CO conversion, CO_2, CH_4, C_2-C_4 and C_{5+} selectivity accounting for all experimental conditions.

4.2. Effects of operating conditions

4.2.1. Effects of H_2/CO feed molar ratio and reaction temperature on conversion and selectivity

The impacts of reaction temperature and the H_2/CO molar ratio on syngas conversion, selectivity of HCs and CO_2 were demonstrated in Figs. 4 (a), (b), (c) and (d), assuming the temperature and H_2/CO ratio in the range of 200 to 257 °C and 1.75 to 2.75 (mole basis), respectively. As it can be seen, the temperature has positive effect on the CO and H_2 conversions (generally syngas conversion); whereas H_2/CO molar ratio has negative impact on total conversion. An increase in the H_2/CO molar ratio from 1.75 to 2.75 reduces the CO conversion and dwindles the CO partial pressure gradient. Decrement of CO partial pressure causes a lower concentration of adsorbed CO, so that more H_2 can be adsorbed and dissociated. As it was expected, the lower concentration of CO leads to a decrease in CO conversion from 47.23 to 36.89 % at 207 °C and from 98.55 to 62.99 % at 257 °C. Decreasing of CO concentration leads to loss of catalytic activity and therefore it causes a decrease in heavy hydrocarbon formation. Therefore it can be concluded that decreasing the H_2/CO molar ratio is favorable due to its effect on conversion of syngas. In contrast, when H_2/CO ratio decreases, the CH_4 selectivity increases and its effect on C_{5+} formation is not considerable. Since the objective is to minimize the CH_4 formation while maximizing CO, H_2 conversion, and C_{5+} selectivity, therefore further investigation on the effects of other operating conditions were carried out to improve the rate of production and conversion.
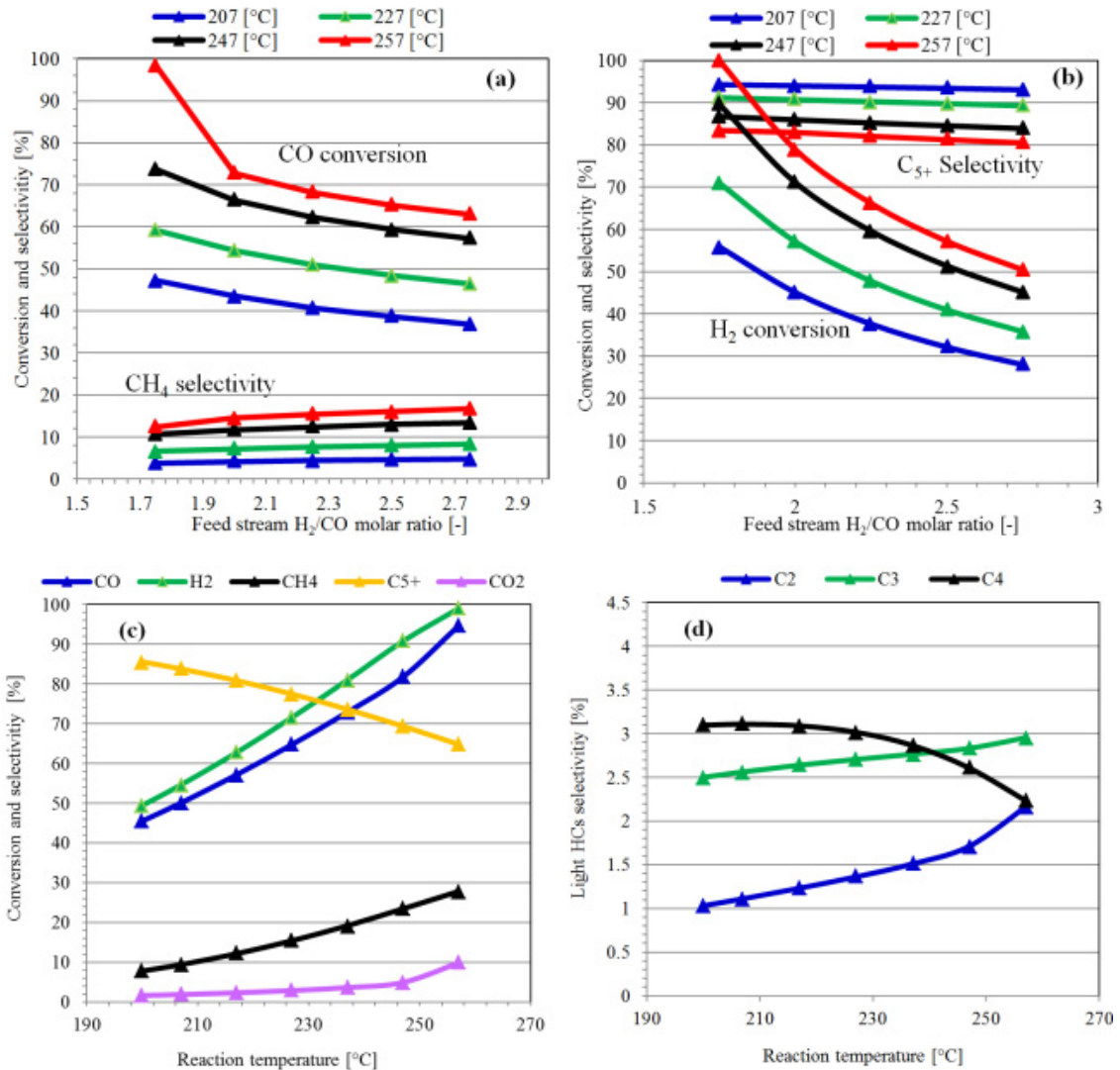
Fig. 4. (a) Effects of the H_2/CO feed stream molar ratio and the reaction temperature on catalytic performance based on CO conversion and CH_4 selectivity at p = 10 bar and GHSV = 3 NL g_{cat}^{-1} h^{-1}. (b) H_2 conversion and C_{5+} selectivity under the same conditions in (a). (c) Effects of the reaction temperature on catalytic performance based on CO and H_2 conversion, CH_4, C_{5+} and CO_2 selectivity at p =15 bar, GHSV = 3 NL g_{cat}^{-1} h^{-1} and H_2/CO = 2/1 (mole basis), (d) Effects of the reaction temperature on C_2-C_4.

4.2.2. Effects of total pressure on conversion and selectivity

FT synthesis can operate at both low and high pressure. At atmospheric pressure, the hydrocarbons are typically in the gaseous state. However, by increasing the total pressure they tend to condense into a liquid; whereas it has a negative influence on CO and H_2 conversion and this attribute was satisfactory outlined in Figs. 5 (a) and (b). An increase in total pressure can be favorable due to its effects on the enhancement of liquid fuel productions. CO and H_2 conversion reduced by 29.2% and 26.5% respectively with an increase of total pressure from 1 to 25 bar. Following changes in total pressure caused a

decriment of CO_2 and C_2-C_4 selectivity by 6.5% and 8.5% respectively and an increase of 10.3% in C_{5+} selectivity. It was clear that the reduction of lighter biofuels' selectivity was due to an increase in the fraction of the liquid products (C_{5+})
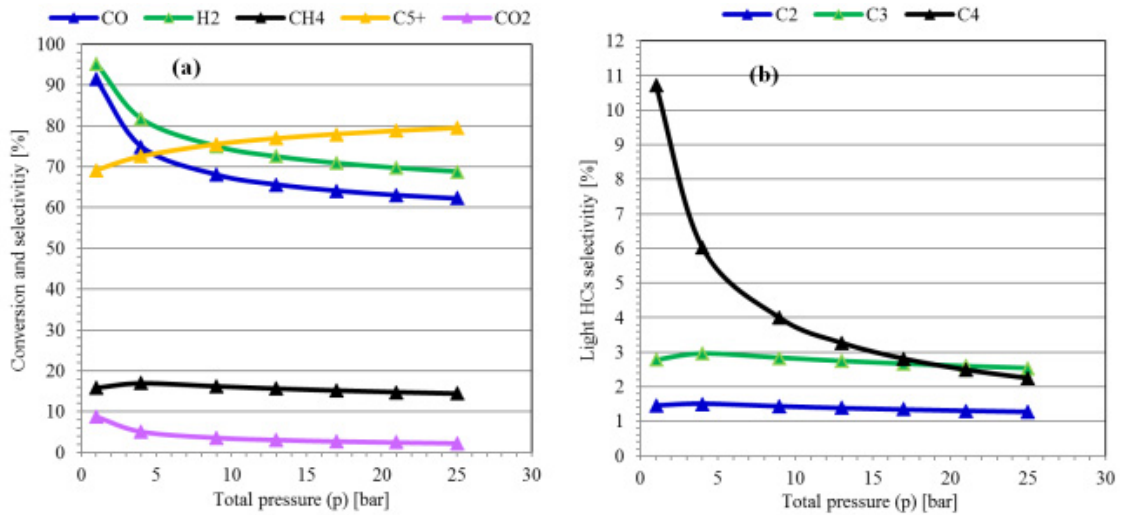

Fig. 5. (a) Effects of the total pressure on catalytic performance based on CO and H_2 conversion, CH_4, C_{5+} and CO_2 selectivity at 227 °C, GHSV = 3 NL g_{cat}^{-1} h^{-1} and H_2/CO = 2/1 (molar basis), (b) Effects of the total pressure on C_2-C_4 selectivity.
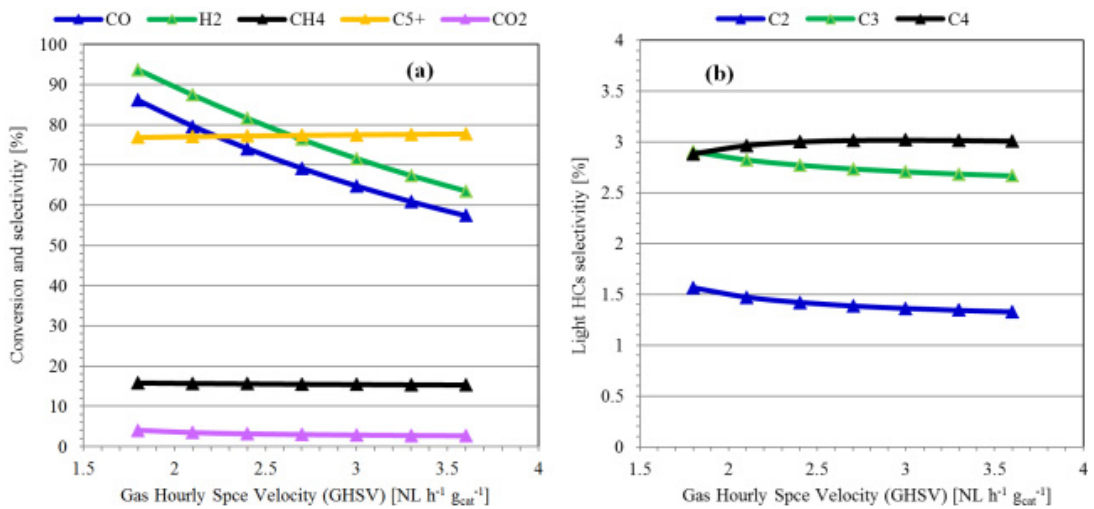

Fig. 6. (a) Effects of the Gas Hourly Space Velocity (GHSV) on catalytic performance based on CO and H_2 conversion, CH_4, C_{5+} and CO_2 selectivity at 227 °C, p = 15 bar and H_2/CO = 2/1 (molar basis), (b) Effects of the GHSV on C_2-C_4 selectivity

4.2.3. Effects of GHSV on conversion and selectivity

Figs. 6 (a) and (b) show the impact of GHSV in the range of 1.8-3.6 NL g_{cat}^{-1} h^{-1}. Changes in the GHSV had a substantial impact on the CO and H_2 conversion because the flow rate corresponded to the inverse of the residence time. Decreases in residence time or enhances of flow rate cause a strong

decrement of CO and H_2 conversion. However, the flow rate did not affect the molecular weight of the hydrocarbons (i.e. CH_4, C_2-C_4 and C_{5+}) that were produced using a cobalt-silica catalyst. The results indicate that at GHSV = 1.8 NL g_{cat}^{-1} h^{-1}, the same reaction temperature and total pressure, the optimal catalyst showed a CO conversion of 86.1% and overall selectivity of 76.8% for heavy hydrocarbons (C_{5+}).

5. Conclusion

A numerical one-dimensional pseudo-homogeneous fixed bed FT synthesis was modeled on a Co-SiO_2 catalyst over simulated N_2-rich syngas. The results predicted by the model were in agreement satisfactorily with the experiments in terms of conversion and selectivity, with the mean absolute relative residuals (MARR) of 13.29%. The results show an increase of the reaction temperature by 57 °C enhanced the catalyst activity in terms of CO and H_2 conversion by up to 50%; whereas its effect on the synthetic bioliquid selectivity was relatively negative, so that the reduction of 20.8% was observed. This reduction was due to an enhancement of the methane selectivity from 7.8 to 27.8%; since an increase in reaction temperature causes a decrease in CO hydrogenation, an increase of the degree of carbidization of the surface and willingness of the surface species to desorb instead of propagating to heavier hydrocarbons. The increased total pressure from 1 to 25 bar resulted in a 6.5 and 8.5% reduction of CO_2 and C_4 selectivity, respectively and an increase of 10.3% in C_{5+} selectivity. It was pointed out that at GHSV = 1.8 NL g_{cat}^{-1} h^{-1} a high CO and H_2 conversion were achieved (86.1 and 93.7%, respectively) while C_{5+} total selectivity was enhanced up to 76.8%. An increase in H_2/CO molar ratio from 1.75 to 2.75 reduces the CO conversion and decreases the CO partial pressure gradient. Decrement of CO partial pressure and its conversion rate causes an increase of H_2 adsorption and dissociation. Consequently, CO conversion was raised from 36.89 to 47.23% at 207 °C and from 62.99 to 98.55% at 257 °C, by decreasing the molar ratio from 2.75 to 1.75.

References

[1] Lee TS, Chung JN. Mathematical Modeling and Numerical Simulation of a Fischer–Tropsch Packed Bed Reactor and Its Thermal Management for Liquid Hydrocarbon Fuel Production using Biomass Syngas. *Energy & Fuels* 2012;**26**:1363-79.

[2] Sheehan J, Camobreco V, Duffield J, Graboski M, Shapouri H. Life Cycle Inventory of Biodiesel and Petroleum Diesel for Use in an Urban Bus. Colorado: *U.S. Department of Energy's Office of Fuels Development*; 1998.

[3] Borg Ø, Dietzel PDC, Spjelkavik AI, Tveten EZ, Walmsley JC, Diplas S, et al. Fischer–Tropsch synthesis: Cobalt particle size and support effects on intrinsic activity and product distribution. *Journal of Catalysis* 2008;**259**:161-4.

[4] Almeida LC, Sanz O, Merino D, Arzamendi G, Gandía LM, Montes M. Kinetic analysis and microstructured reactors modeling for the Fischer–Tropsch synthesis over a Co–Re/Al2O3 catalyst. *Catalysis Today* 2013;**215**:103-11.

[5] Atashi H, Mansouri M, Hosseini S, Khorram M, Mirzaei A, Karimi M, et al. Intrinsic kinetics of the Fischer-Tropsch synthesis over an impregnated cobalt-potassium catalyst. *Korean J Chem Eng* 2012;**29**:304-9.

[6] Marvast MA, Sohrabi M, Zarrinpashne S, Baghmisheh G. Fischer-Tropsch Synthesis: Modeling and Performance Study for Fe-HZSM5 Bifunctional Catalyst. *Chemical Engineering & Technology* 2005;**28**:78-86.

[7] Mirzaei AA, Shirzadi B, Atashi H, Mansouri M. Modeling and operating conditions optimization of Fischer–Tropsch synthesis in a fixed bed reactor. Journal of Industrial and Engineering Chemistry 2012;**18**:1515-21.

[8] Mogalicherla AK, Elbashir NO. Development of a Kinetic Model for Supercritical Fluids Fischer−Tropsch Synthesis. *Energy & Fuels* 2011;**25**:878-89.

[9] Park N, Kim J-R, Yoo Y, Lee J, Park M-J. Modeling of a pilot-scale fixed bed reactor for iron-based Fischer–Tropsch synthesis: Two-dimensional approach for optimal tube diameter. *Fuel* 2014;**122**:229-35.

[10] Rafiq MH, Jakobsen HA, Schmid R, Hustad JE. Experimental studies and modeling of a fixed bed reactor for Fischer–Tropsch synthesis using biosyngas. *Fuel Processing Technology* 2011;**92**:893-907.
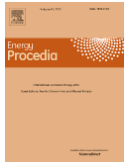
Biography

Nima Moazami was born in Tehran, Iran, in 1988. He received his MEng degree in Mechanical Engineering by achieving First-Class Honors from the University of Birmingham, Birmingham, UK, in 2011. He has been awarded The University of Birmingham School Full-Scholarship to fund his Ph.D. research programme with supervision from Prof. Miroslaw L. Wyszynski since November 2011.